NOTICE

The quality of this microform is heavily dependent upon the quality of the original thesis submitted for microfilming. Every effort has been made to ensure the highest quality of reproduction possible.

If pages are missing, contact the university which granted the degree.

Some pages may have indistinct print especially if the original pages were typed with a poor typewriter ribbon or if the university sent us an inferior photocopy.

Reproduction in full or in part of this microform is governed by the Canadian Copyright Act, R.S.C. 1970, c. C-30, and subsequent amendments.

AVIS

La qualité de cette microforme dépend grandement de la qualité de la thèse soumise au microfilmage. Nous avons tout fait pour assurer une qualité supérieure de reproduction.

S'il manque des pages, veuillez communiquer avec l'université qui a conféré le grade.

La qualité d'impression de certaines pages peut laisser à désirer, surtout si les pages originales ont été dactylographiées à l'aide d'un ruban usé ou si l'université nous a fait parvenir une photocopie de qualité inférieure.

La reproduction, même partielle, de cette microforme est soumise à la Loi canadienne sur le droit d'auteur, SRC 1970, c. C-30, et ses amendements subséquents.

Canada

CONFINED FLOW PAST OVERSIZED BLUFF BODIES

Peter Aberg

A Thesis

in

The Department

of

Civil Engineering

Presented in Partial Fulfillment of the Requirements
for the Degree of Master of Engineering at
Concordia University
Montreal, Quebec, Canada

July 1989

ISBN 0-315-51364-0

ABSTRACT

CONFINED FLOW PAST OVERSIZED BLUFF BODIES

Peter Aberg

The characteristics of two-dimensional non-cavitating flow past oversized triangular prisms are studied. The separation pressure coefficient and the vortex shedding frequency are obtained. The separating streamline velocity is used to form the Strouhal numbers to absorb blockage effects. At the higher blockages the separating streamline velocity is found to be different from the contracted jet velocity. Furthermore, the values of Strouhal number decrease considerably at very high blockages. Besides the flow past the prism, limited studies related to flow past a flat plate and a gate subject to high blockages are also reported to provide a comparative study of the flow characteristics.

ACKNOWLEDGEMENTS

I wish to express my appreciation to Dr. A. S. Ramamurthy and Dr. B. L. Carballada for suggesting the thesis topic and for their guidance in the course of the investigation. I am indebted to R. Balachandar for essential discussion and for his assistance in the experimental component of this thesis. Many thanks are also due to Diep Ngoc Vo who offered important technical support. Finally, I am very grateful to my wife, without whose support this thesis would never have been completed.

TABLE OF CONTENTS

LIST OF FIGURES

LIST OF TABLES

NOTATIONS

B = width of test section

b = width of bluff body

b/B = blockage ratio

C_c = contraction coefficient

C_d = drag coefficient

C_{dj} = drag coefficient normalized by u_j

C_{ps} = separation pressure coefficient

d = distance between free streamlines

f = vortex shedding frequency

K_j = variable ($=u_j/u$)

K_s = empirical variable ($=u_s/u$)

P = pressure of undisturbed flow

P_s = separating pressure

Re = Reynolds number

S = Strouhal number

S_j = Strouhal number normalized by u_j

S_s = Strouhal number normalized by u_s

S^* = universal Strouhal number

u = mean velocity upstream of the body

u_j = contracted jet velocity

u_s = separating streamline velocity

θ = orientation

ν = kinematic viscosity

ρ = density of fluid

NON-DIMENSIONAL TEST VARIABLES

The following non-dimensional test variables are used in this thesis.

(i) Blockage:

$$\frac{b}{B} \qquad (1)$$

where,

b = width of the test body

B = width of the test section

(ii) Reynolds number:

$$Re = \frac{u\,b}{\nu} \qquad (2)$$

where,

u = free stream velocity

ν = kinematic viscosity

(iii) Strouhal number:

$$S = \frac{f\,b}{u} \qquad (3)$$

where,

f = vortex shedding frequency

(iv) Strouhal number normalized by the separating streamline velocity:

$$S_s = \frac{f\,b}{u_s} \qquad (4)$$

where,

u_s = separating streamline velocity

(v) Strouhal number normalized by the contracted jet velocity:

$$S_j = \frac{f\,b}{u_j} \qquad (5)$$

where,

u_j = contracted jet velocity

(vi) Universal Strouhal number:

$$S^* = \frac{f\,d}{u_s} \qquad (6)$$

where,

d = wake width

(vii) Variable:

$$K_j = \frac{u_j}{u} = \frac{1}{(1 - \frac{b}{B}) C_c} \qquad (7)$$

where,

C_c = contraction coefficient (Eq. 10)

(viii) Empirical variable:

$$K_s = \frac{u_s}{u} \qquad (8)$$

(ix) Separation pressure coefficient:

$$C_{ps} = \frac{P_s - P}{\frac{1}{2} \rho u^2} = 1 - K_s^2 \qquad (9)$$

where,

P_s = separating pressure

(x) Contraction coefficient:

$$C_c = \frac{\pi}{\pi + R \tan^{-1} \frac{2}{R}} \qquad (10)$$

where,

$$R = \frac{[\,1 - ((1 - \frac{b}{B})\, C_c)^2\,]}{(1 - \frac{b}{B})\, C_c}$$

INTRODUCTION

Pressure coefficients and Strouhal numbers for two-dimentional bodies of several shapes in normal, uniform flows are readily available in the literature [Roshko (1953), Hoerner (1965), Shaw (1969, 1971a, 1971b)]. These studies deal with unconstrained or lightly constrained flow past bluff bodies. Equivalent details for flow which are highly constrained are not as readily available, although there is a frequent need for the same.

The present experimental investigation deals with the characteristics of two-dimensional non-cavitating flow past oversized sharp-edged bodies. Here, the term "oversized" relates to the situation when the test body size is comparable to the test section size. The ratio of the model area to the test section area is denoted as blockage. In the present study, depending on the blockage ratio, the flow past bluff bodies are denoted as lightly constrained ($b/B < 0.23$), moderately constrained ($0.23 \leq b/B \leq 0.58$) and highly constrained ($b/B > 0.58$).

The present study was carried out to provide basic data related to flow past bluff bodies in highly constrained flows. The results of this study should be of interest in the design of gate valves in closed conduits. In the design of gates, avoiding the resonance between the vortex formation frequency and the natural frequency of the system is important. Other applications include the study of flow behaviour past large pillars placed in the path of an air duct.

CHAPTER 1

Review of previous investigations

In this chapter, studies relating to the characteristics of flow past partially constrained two-dimensional sharp-edged bluff bodies are reviewed. Although a considerable number of studies exist for the lower blockages [Roshko (1953), Abernathy (1962), Shaw (1971b), Toebes (1971), Modi and El-Shirbiny (1977), Ramamurthy et. al. (1973a, 1973b, 1989)], few studies have dealt with large blockages. A comprehensive compilation of data related to flow past sharp-edged bluff bodies is provided in Table 1 to enable the designer to obtain information about the separation pressure coefficient C_{ps} and the vortex shedding frequency.

Tozkas (1965) conducted exploratory studies relating to the vortex shedding frequency behind flat plates up to a blockage of 0.78. Using the same maximum blockage, Chen (1967) measured the separation pressure coefficient for flow past a flat plate. The vortex shedding frequency behind a 90° prism up to a blockage of 0.71 were also obtained by Chen. Both Tozkas and Chen found the "universal" Strouhal number S^* not to be independent of blockage. For a multiple body configuration of triangular prisms at 0°, Lee (1973) had difficulty in detecting a dominant frequency for $0.61 \leq b/B \leq 0.74$. For the same configuration, the Strouhal number S_j normalized by the contracted jet velocity u_j was found to be almost constant up to a blockage of 0.30.

Ng (1972) determined the drag coefficient C_d for triangular prisms at 0° up to a blockage of 0.71. He concluded that the drag coefficient normalized by the contracted jet velocity C_{dj} will be independent of blockage. Further, according to his studies, S_j for the same prism was constant up to a blockage of 0.30 and increased beyond this blockage.

Ramamurthy et. al. (1989) pointed out that C_d of constrained bluff bodies at large

blockages can be evaluated without recourse to empirical relations by using a simplified momentum analysis which yields,

$$C_d = \frac{B}{b}(K_j - 1)^2 \qquad (11)$$

where, K_j is the ratio of the contracted jet velocity to the free stream velocity. Eq.(11) is suggested to be valid when blockage is greater than 0.30.

Shaw (1969, 1971a) and Ramamurthy et. al. (1989) indicated that u_j is approximately equal to the separating streamline velocity u_s for a flat plate when blockage is only moderate. At lower blockages, u_j was found to be different from u_s. Presently, no information is available to compare the separating streamline velocity u_s and the contracted jet velocity u_j at very large blockages.

Scope of the present study

With few exceptions, the majority of studies reviewed above are concerned with flows which are termed lightly constrained (low blockage) and moderately constrained (moderate blockage). The purpose of this investigation is to extend the present knowledge of the effects of wall interference on the hydrodynamic characteristics in highly constrained flows (b/B > 0.58). This investigation, however, is limited to sharp-edged bluff bodies such as flat plates, 0° prisms and wall mounted gates.

The test models investigated were centrally mounted triangular 0° prisms with fixed separation edges (Fig.3). This shape was chosen to reduce Reynolds number effects [Ramamurthy et. al. (1989)]. The study was particularly concerned with the properties of

the vortex shedding frequency and the separation pressure coefficient for high blockages. The dominant frequency of pressure pulsations were obtained from power spectra from which the Strouhal number could be determined.

An experiment was also carried out to study the similarities between the vortex shedding mechanism for a gate (b/B = 0.94) as compared to a prism in highly constrained flow. Furthermore, to study the possibility of afterbody effects of the prism at high blockages, flow past a flat plate (b/B=0.93) was also investigated. Typical power spectra for the different model shapes at various blockages are shown in Figs. 16-19. Attempts were made to eliminate blockage effects by normalizing the Strouhal number using separating streamline velocity as a velocity scale.

CHAPTER 2

Experimental set-up and procedures

The experiments were carried out in a water tunnel, consisting of a large rectangular settling chamber which contracts smoothly to a rectangular test section. The settling chamber was adopted to reduce the turbulence level in the test section and provide flow condition which is nearly two-dimensional. The test section was 508.0 mm in length, 154.0 mm in height and 4.76 mm in width. Visual observation was made possible through a plexiglas window on the front of the test section. For details of the test section see Balachandar (in preparation).

The triangular prism models made of brass were centrally mounted and spanned the whole width of the test section. The model surfaces were polished to a smooth finish. The prisms were always positioned with the front face normal to the flow, denoted as 0° orientation (Fig. 3). The different blockages tested ranged from 0.24 to 0.93. The stagnation pressure P_{stg} was measured using a pressure tap (0.5 mm in diameter) located at the center of the front face, while the two separation pressures P_s were measured by pressure taps located close to the two separating corners of the model.

The vortex shedding frequency was obtained using pressure transducers [Validyne, DP 15] connected to a Fast Fourier Transform Analyser [Wavetek, 5830-A] through a transducer demodulator [Validyne, CD 15] to carry out the spectral analysis The transducers were located close to the edge of the separating streamline (Fig. 2). The associated instrumentation is shown in Fig. 4. The discharge was measured with the help of a 60° triangular notch weir. The accuracy of measurements are given in Appendix I.

At a later stage in the experimental program, it was decided to add two more models: A gate attached to the lower wall and a flat plate centrally mounted normal to the flow.

Both models were fabricated in aluminum and polished to a smooth finish (Fig. 3).

CHAPTER 3

Presentation of results

The theoretical variation of K_j for $0 \leq b/B \leq 0.50$ is shown in Fig. 5. Values of the contraction coefficient C_c for a flat plate are known for any blockage and hence K_j can be estimated (Eq. (10)). Fig. 5 also indicates the variation of the experimental values of $K_s = (1 - C_{ps})^{0.5}$ obtained from the present investigation and several other previous studies. Shaw (1971a) and Ramamurthy et. al. (1989) have indicated that the contracted jet velocity u_j is not equal to the free streamline velocity u_s at very low blockages. Fig. 5 shows that as the blockage tends to 0, K_j approaches 1.0 and the value of K_s is about 1.46. For $0.20 \leq b/B \leq 0.50$, K_s is approximately equal to K_j. The values of K_s for 0° prisms obtained in the present study are in good agreement with those obtained by previous studies (Fig. 5).

In the present investigation the Reynolds number range ($1.4 \times 10^5 - 5.6 \times 10^5$) was chosen to cover most practical applications. Both C_{ps} and S for the prism were found to be independent of Re for all blockages tested except at very large blockages and very low values of Re (Figs. 6-11). The results related to the flat plate and the gate show a minor scatter in C_{ps} and S when plotted against Re (Figs. 8 and 11). Tables 2-12 show the variation of C_{ps} and S with Re for the different models tested in the present investigation.

Fig. 12 shows the variation of K_j and of K_s for $0.50 \leq b/B \leq 0.93$. The experimental values of K_s for prisms obtained in the present study and the values of K_s for flat plates reported by Chen (1967) follow the trend of K_j at blockages up to approximately 0.70. However, at extremely high blockages ($b/B > 0.70$) K_s clearly deviates from K_j. It appears that as the blockage increases the difference between K_s and K_j also increases. Plotted in Fig. 12 are also the values of K_s obtained for the flat plate and the gate. The behaviour of flow past these two shapes are expected to be quite different.

The variation of Strouhal number for $0 \leq b/B \leq 0.50$ is shown in Fig. 13. The figure indicates that as blockage increases the value of S also increases. The data obtained from the prisms in the present study concur with those reported in previous studies. Fig. 14 indicates that the values of S for the prisms in the present investigation deviate from the expected trend as the blockage increases above 0.60. For $0.82 \leq b/B \leq 0.93$, the values of Strouhal number show a decreasing trend. There is also a pronounced scatter in the Strouhal number for the very high blockages. Tozkas (1965) reported a slightly decreasing trend of S in the blockage range of 0.50 - 0.78 (Fig. 14). These values show a lower trend than the values of S obtained in the present study. Since his studies were only exploratory in nature one should seek a qualitative agreement of his data with present results.

Fig. 14 also shows that the values of Strouhal number for the gate (Fig. 3) and the flat plate (Fig. 3) are shown for a specific value of b/B=0.94 and b/B=0.93 respectively. Although the flow characteristics past the wall body such as the gate is quite different from the characteristics of flow past a centrally mounted prism at the high blockage of 0.93, the value of S appears to be nearly the same for both shapes. Furthermore, the flat plate with no significant afterbody seems to have a value of S which is close to that of the prism at this high blockage.

The values of separation pressure coefficient for the gate and the flat plate are found to be lower than those for the prism at b/B=0.93 (Figs. 7 and 8). C_{ps} values for the gate show a significantly lower trend than for the prism.

CHAPTER 4

Discussion of results

The experimental values of K_s are obtained from energy considerations by assuming the invariance of velocity along the free streamline up to the region where the wake reaches its maximum width (Fig. 2). This assumption has been taken for granted in the classical free streamline theory [Robertson (1965)].

Results from the present study (Fig. 12) show that the values of K_s deviates from K_j at the very high blockages ($b/B > 0.70$). This is an indication of a difference between the separating velocity and the contracted jet velocity in this blockage range. It appears that the contraction of the jet is not as steep as one would expect. As the gap width becomes smaller, one can expect the boundary layer thickness and its influence on the flow behaviour to become more important.

Fig. 14 shows a scatter in the Strouhal numbers for the 0° prism for very high blockages at low values of Re. This could be explained by a less stable vortex formation behind the body for these blockages. In the power spectra obtained, it was sometimes hard to detect a distinct dominant frequency. Strouhal number data obtained by Lee (1973) indicated a similar problem at very large blockages. Tozkas (1965) and Chen (1967) reported that the velocity fluctuation in the wake became increasingly irregular with increasing blockage for a flat plate and a 90° prism respectively.

In the present investigation, visual observations were carried out by letting the flow cavitate mildly. These observations indicate an alternate vortex formation resulting from an interaction of the two shear layers leading to the formation of the Karman vortex street for blockages up to approximately 0.50. It was also observed that there was no clear indication of the formation of the Karman vortex street behind the prism in highly

constrained flows. The vortex shedding frequency obtained behind the gate was found to be nearly identical to that of the prism and the flat plate at the same blockage. This clearly indicates that there is no interaction between the two shear layers for the prism and the flat plate at the very high blockages. Fig. 14 shows that at a blockage around 0.80, S reaches its maximum value and begins to decrease as b/B is increased. It is possible that the Karman vortex street becomes less dominant or fails to exist at all at this blockage. The values of S obtained by Tozkas (1965), showing a significantly lower trend, is probably the result of an imperfect spectral measurement as pointed out by Chen (1967). Nevertheless, qualitatively, Tozkas' data share the same profile as the present results. Shaw (1971b) investigated the vortex frequency when a flat plate was progressively moved from the center of the conduit towards the wall. Even though the largest blockage tested was 0.22, it is interesting to note that S first increased, but when the gap between the plate and the wall became very small S decreased. Furthermore, when the gap became negligible S reached approximately the center line value, i.e. S was approximately the same for a centrally mounted plate as for a gate. He claimed that the vortex shedding from the gate was less dominant because of the absence of Karman vortex formation.

Efforts were made to normalize the obtained values of S for the prisms using u_s as a velocity scale (S_s= fb/u_s). Fig. 15 shows that in lightly constrained flow (b/B < 0.23), the blockage effects are absorbed when the frequency is normalized by the separating streamline velocity. For moderately constrained bodies (0.23 ≤ b/B ≤ 0.58) S_s indicates an increasing trend and in highly constrained flow S_s drops sharply. This is not surprising in view of the vortex formation process being different at higher blockages.

In Figs. 7 and 8 the lower Cps values obtained for the plate compared to the prism of the same blockage (b/B=0.93) leads to the speculation that there is a significant afterbody effect for the prism in highly constrained flow. The afterbody is almost analogous to the effect of providing a splitter plate behind a flat plate leading to increasing values of back

pressure and consequently decreasing values of -Cps. Several experimental investigations have been carried out placing a splitter plate behind a bluff body [Hoerner (1965), Roshko (1953), Bhaskaran. (1977)]. Results from these studies show that the vortex shedding frequency decreases, values of Cps increases, and the drag coefficient consequently decreases.

CHAPTER 5

Conclusions

(i) Results for a 0° prism at very high blockages (b/B > 0.70) show that the separating streamline velocity was different from the contracted jet velocity.

(ii) Visual observations indicated that no Karman vortex street was present behind the 0° prism in highly constrained flow. Furthermore, comparing the results relating to the gate (b/B=0.94) with those of the prism (b/B=0.93) show that the Strouhal numbers are nearly identical. This indicates that there is no interaction between the two shear layers for a 0° prism at the very high blockages.

(iii) The values of the separation pressure coefficient obtained for the flat plate were found to be lower than those obtained for the 0° prism at the same blockage (b/B=0.93). It is suggested that there is a significant afterbody effect for a 0° prism compared to a flat plate in highly constrained flow.

Scope for further investigations

The present study was limited to the characteristics of non-cavitating flow past 0° prisms at high blockages. Further research is called for investigating triangular prisms at different angles in highly constrained flow. Moreover, cavitating flow past bluff bodies for the higher blockages needs to be investigated.

REFERENCES

Abernathy, F. H., "Flow over an inclined plate", Journal of Basic Engineering, Transactions of the ASME, Sept., 1962, pp. 380-388.

Awbi, H.B., "Wind-tunnel-wall constraint on two-dimensional rectangular-section prisms", Journal of Industrial Aerodynamics, 3 (1978) 285-306.

Balachandar, R., "Cavitation characteristics in constrained separating flows", Doctoral thesis, Concordia University, Montreal, (in preparation).

Bhaskaran, P., "Characteristics of flow past bluff cavitating sources", Doctoral thesis, Department of Civil Engineering, Concordia University, Montreal, 1977.

Chen, Y. S., "Effect of confining walls on the periodic wake of 90-degree wedges", Master's thesis, Department of Mechanics and Hydraulics, University of Iowa, 1967.

Courchesne, J., and Laneville, A., "A comparison of correction methods used in the evaluation of drag coefficient measurements for two-dimensional rectangular cylinders", Journal of Fluids Engineering, Transactions of the ASME, Dec., 1979, Vol. 101, pp. 506-510.

Hoerner, S. F., "Fluid dynamic drag", published by the author, 1965.

Lee, P.M., "Boundary effects on flow past bluff bodies", Doctoral thesis, Faculty of Engineering, Sir George Williams University, Montreal, 1973.

Modi, V.J., and El-Shirbiny, S. E., "A free-stream line model for bluff bodies in confined flow", Journal of Fluids Engineering, Transactions of the ASME, Sept., 1977, pp. 585-592.

Ng, C. P., "Wall interference effects on steady force co-efficients of bluff bodies", Master's thesis, Faculty of Engineering, Sir George Williams University, Montreal, 1972.

Ramamurthy, A.S., and Bhaskaran, P., "Constrained flow past cavitating bluff bodies", Journal of Fluids Engineering, Transactions of the ASME, Vol 99, No.4,1977, pp.717-726.

Ramamurthy, A.S., and Lee, P.M., "Wall effects on flow past bluff bodies", Journal of Sound and Vibrations, Vol 31(4), 1973a, pp.443-451.

Ramamurthy, A.S., and Ng, C.P., "Effect of blockage on steady force coefficients", Journal of Engineering Mechanics Division, Proceedings of the ASCE, Vol. 99, No.EM4, Aug., 1973b.

Ramamurthy, A. S., Balachandar, R., and Diep Ngoc Vo, "Blockage correction for sharp edged bluff bodies", Journal of Engineering Mechanics Division, Proceedings of the ASCE, Vol. 115, No. 7, July, 1989, pp. 1569-1567.

Robertson, J. M., "Hydrodynamics in theory and application", Prentice Hall Inc., New Jersey, 1965.

Roshko, A., "On the drag and shedding frequency of two-dimensional bluff bodies", NACA, TN 3169, 1953.

Shaw, T.L., "Steady flow past flat plate in channel", Journal of the Hydraulics Division, Proceedings of the ASCE, HY 6, Nov., 1969, pp. 2013-2028.

Shaw, T.L., "Effect of side walls on flow past bluff bodies", Journal of the Hydraulics Division, Proceedings of the ASCE, HY1, Jan., 1971a, pp. 65-79.

Shaw, T. L., "Wake dynamics of two-dimentional structures in confined flows", Proceedings, 14th Congress of the IAHR, Paris, Vol. 2, B 6, 1971b, pp. 41-48.

Simmons, J.E.L., "The relationship between the base pressure on a bluff body and the velocity at separation", Aeronautical Journal, July, 1974, pp. 330-331.

Sullerey, R.K., Gupta, A.K. and Moorthy, C.S., "Similarity in the turbulent near wake of bluff bodies", AIAA Journal, Vol. 13, No.11, Nov., 1975, pp. 1425-1429.

Toebes, G.H., "The frequency of oscillatory forces acting on bluff cylinders in constricted passages", Proceedings, 14th Congress of the IAHR, Paris, Vol. 2, B 7, 1971, pp. 49-58.

Tozkas, A., "Effect of confining walls on the periodic wake of cylinders and plates", Master's thesis, Department of Mechanics and Hydraulics, University of Iowa, 1965.

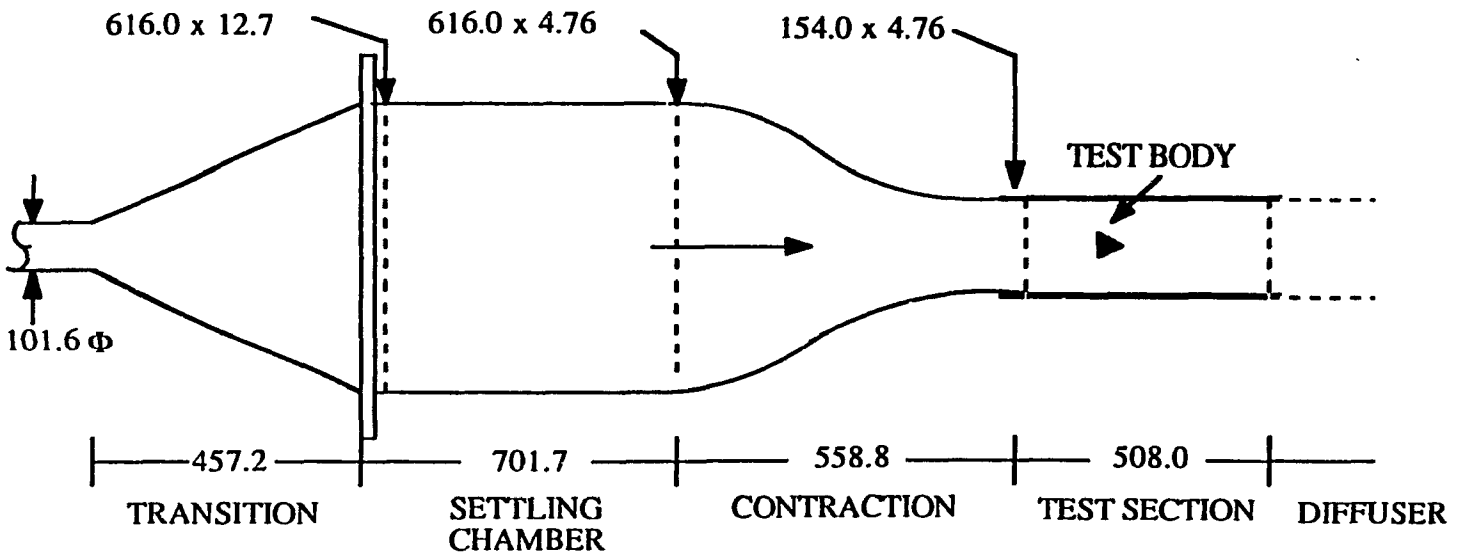

(Not to scale. All dimensions in millimeters)

Fig. 1 Front elevation of water tunnel test set-up

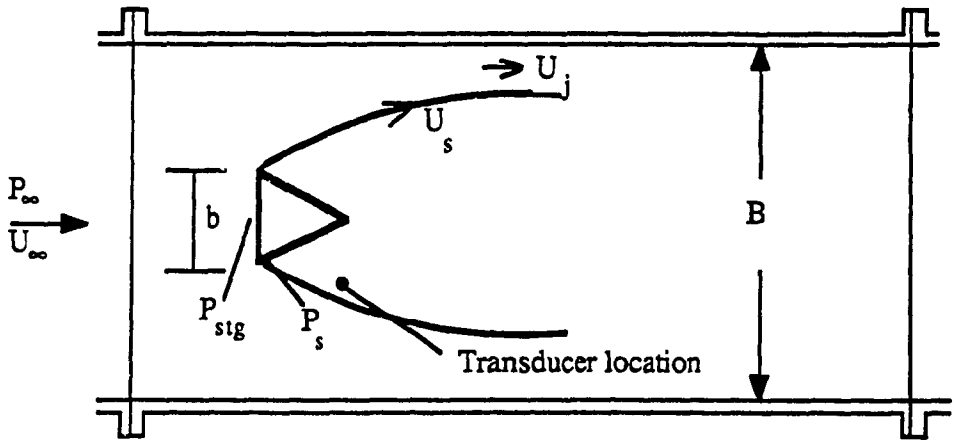

Fig.2 Test section

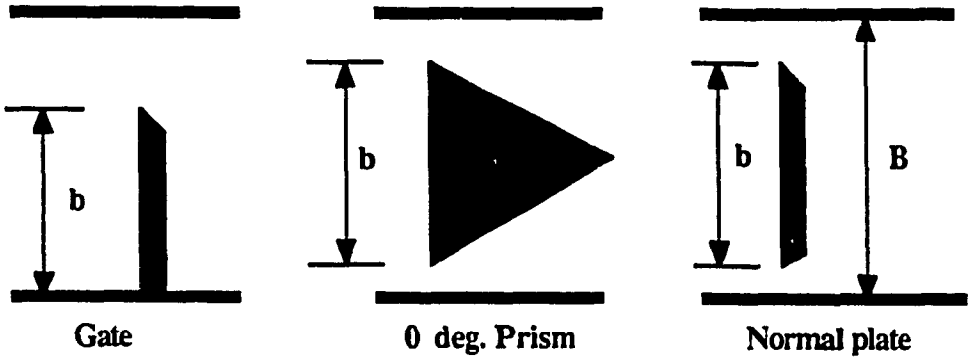

Fig.3 Model shapes tested

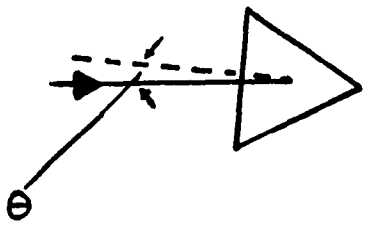

Fig. 3 (continued). θ orientation for a prism

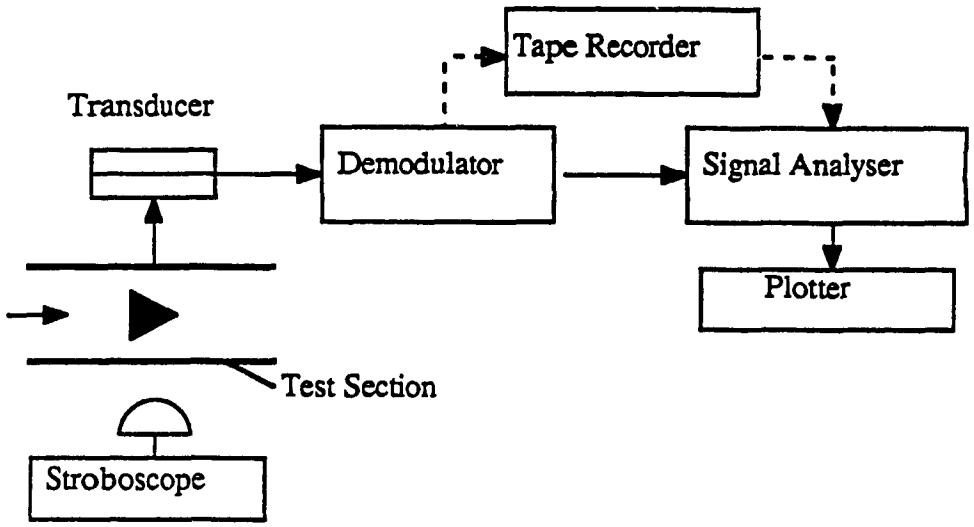

Fig.4 Instrumentation

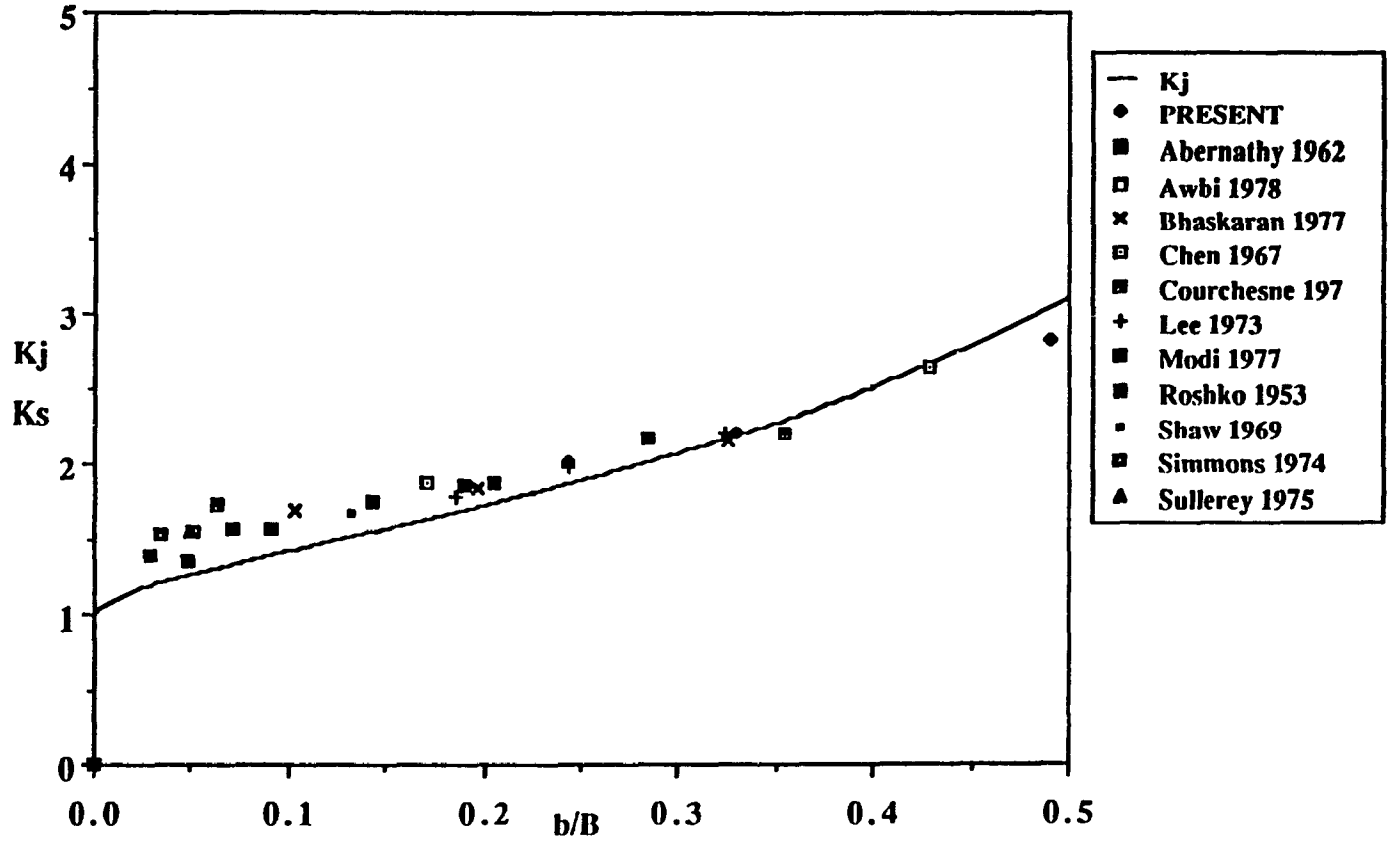

Fig. 5 Variation of K_j and K_s with blockage for sharp-edged bluff bodies ($b/B < 0.5$)

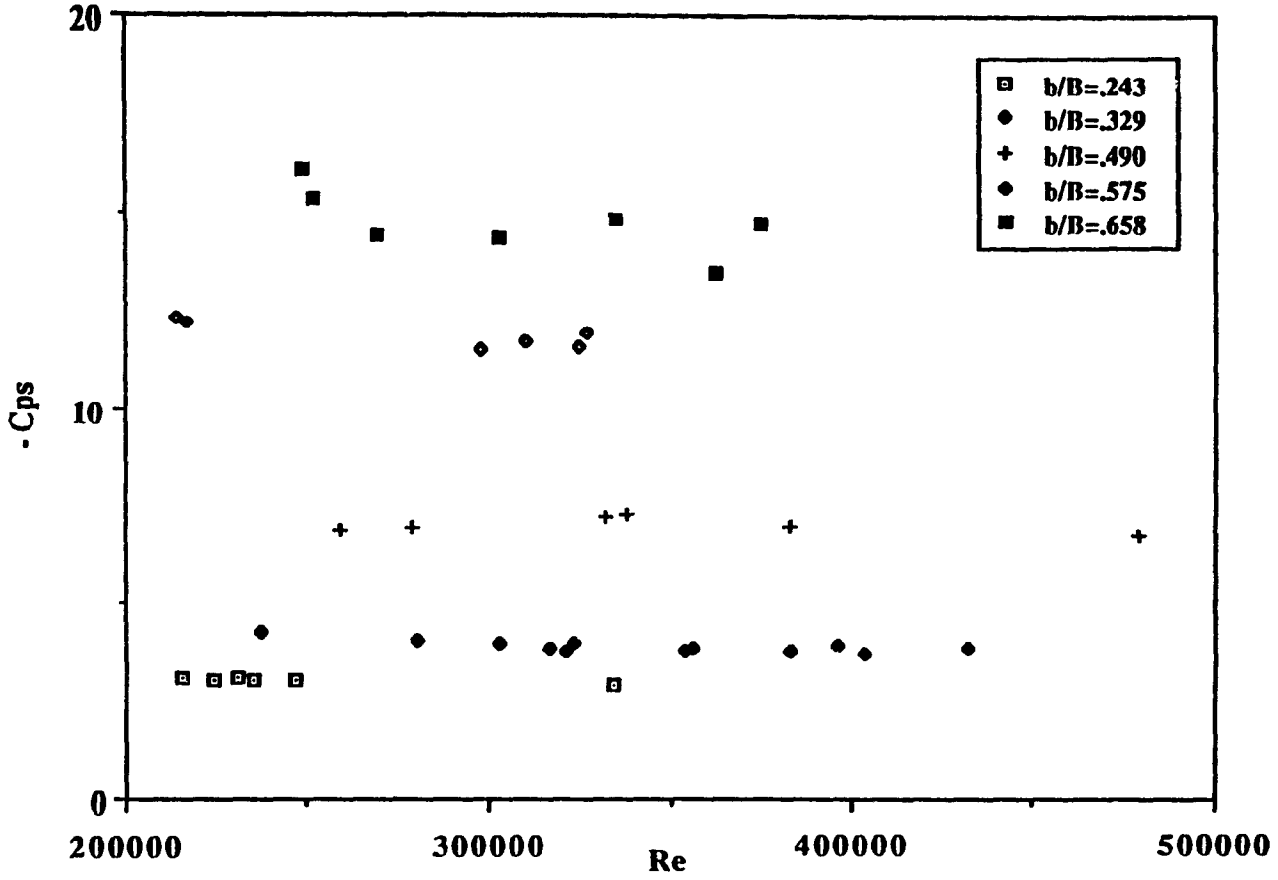

Fig. 6 Variation of C_{ps} with Re for 0° prism ($0.243 \leq b/B \leq 0.658$)

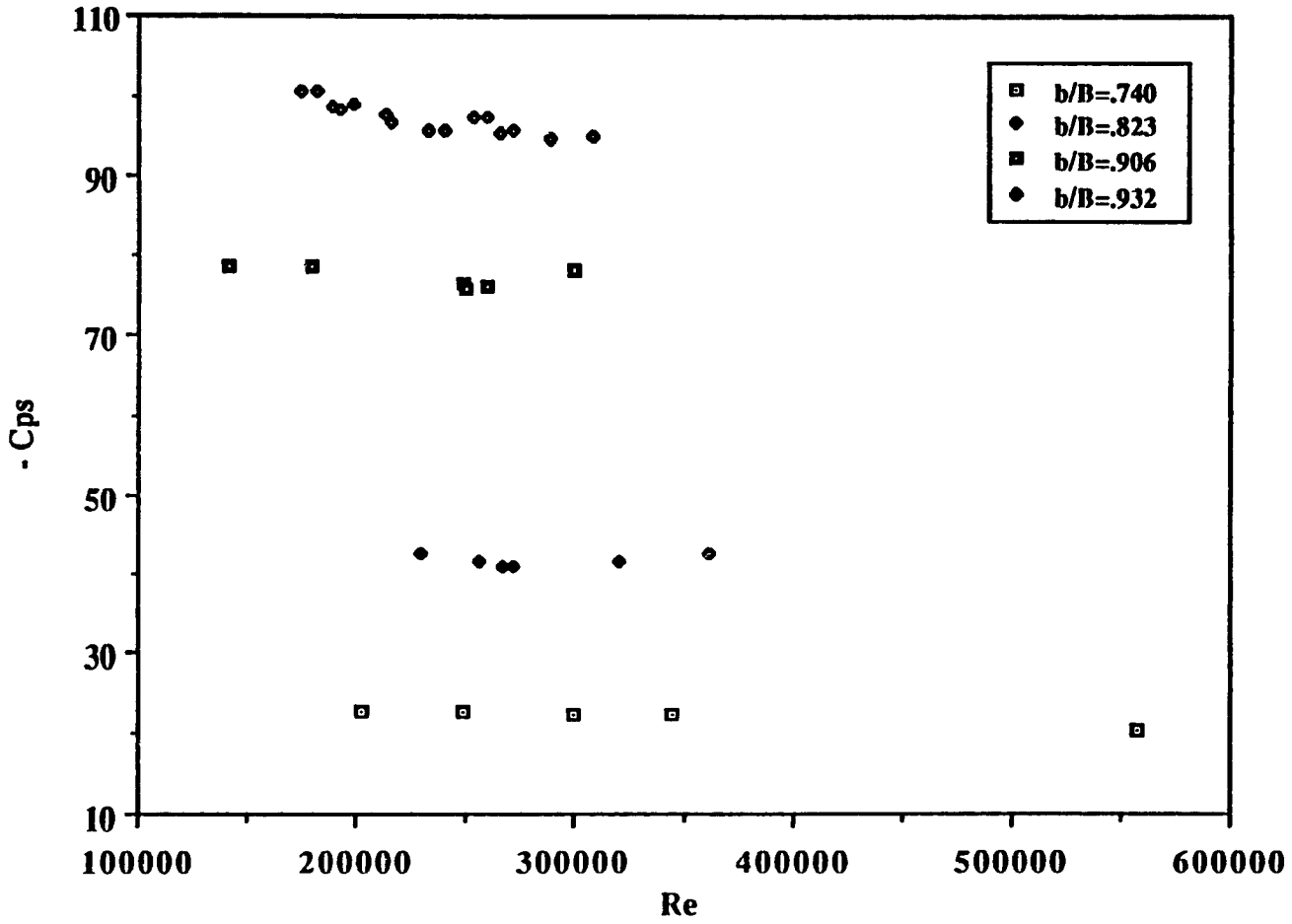

Fig. 7 Variation of C_{ps} with Re for 0° prism ($0.740 \leq b/B \leq 0.932$)

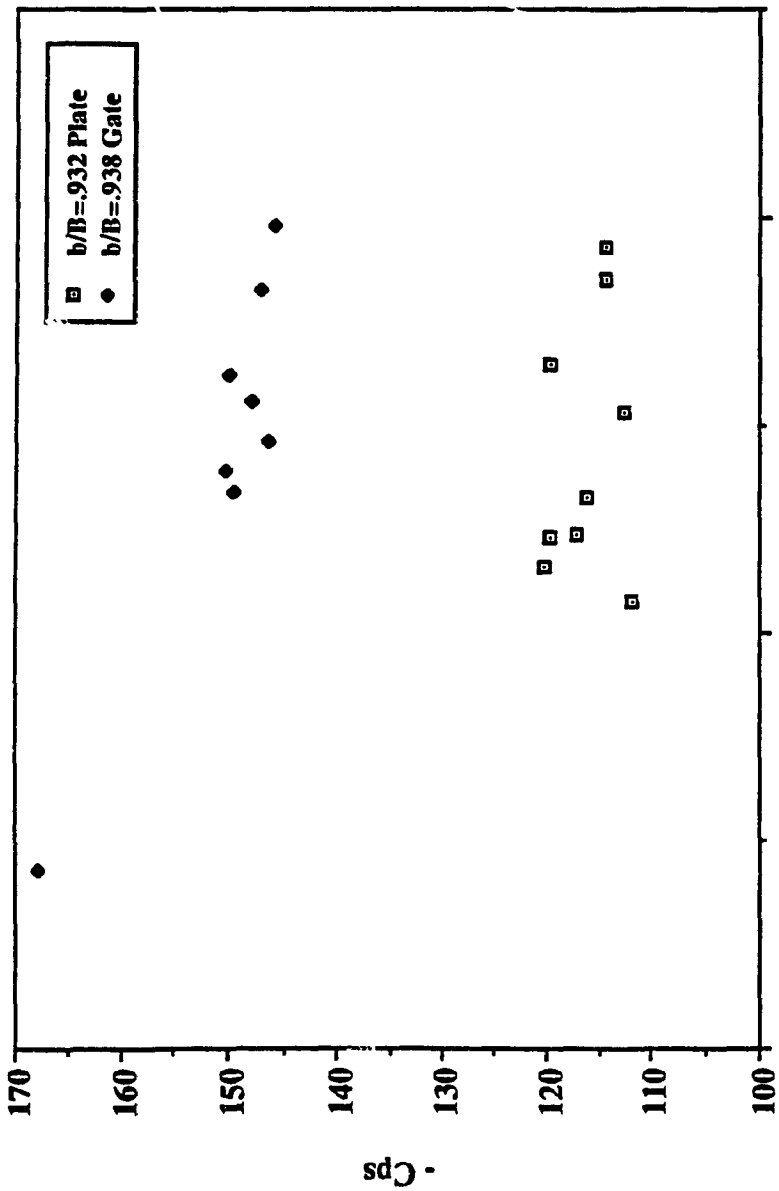

Fig. 8 Variation of C_{ps} with Re for flat plate and gate

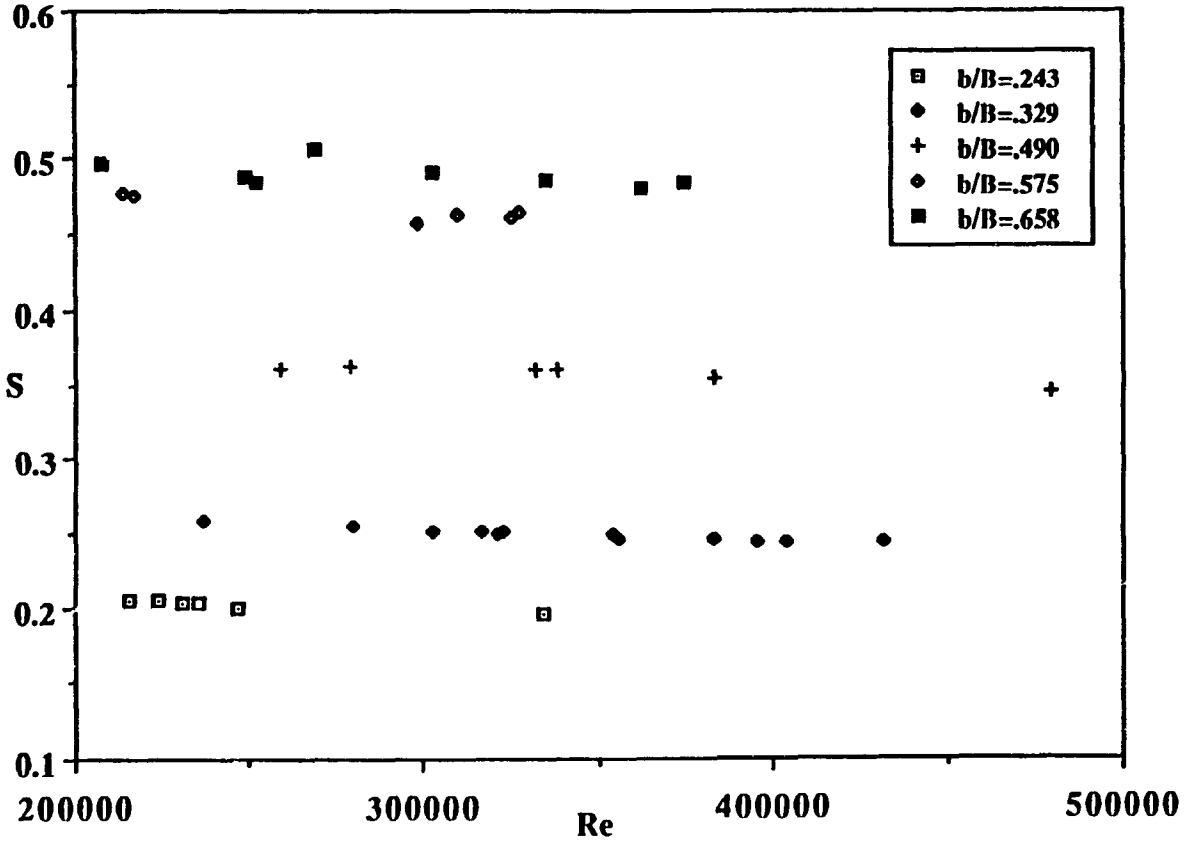

Fig. 9 Variation of S with Re for 0° prism ($0.243 \leq b/B \leq 0.658$)

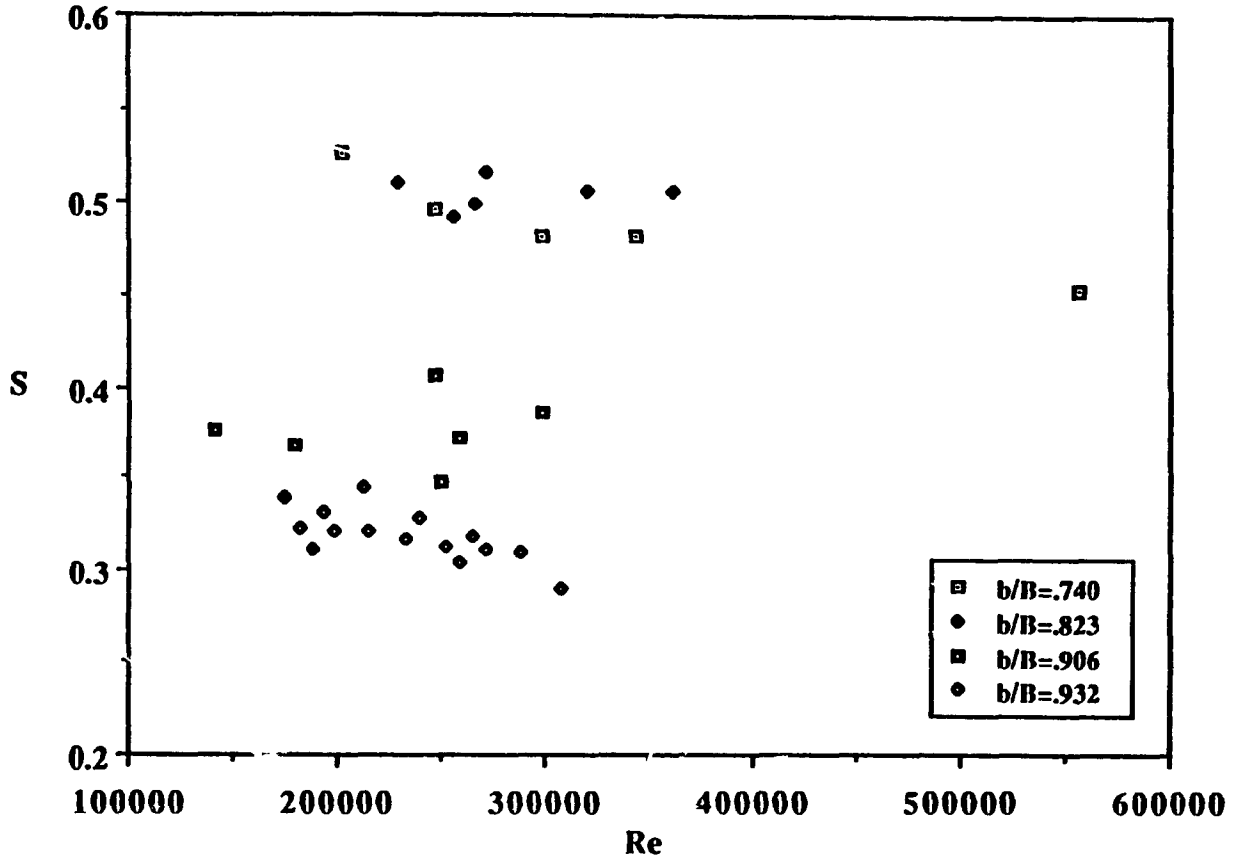

Fig. 10 Variation of S with Re for 0° prism ($0.740 \leq b/B \leq 0.932$)

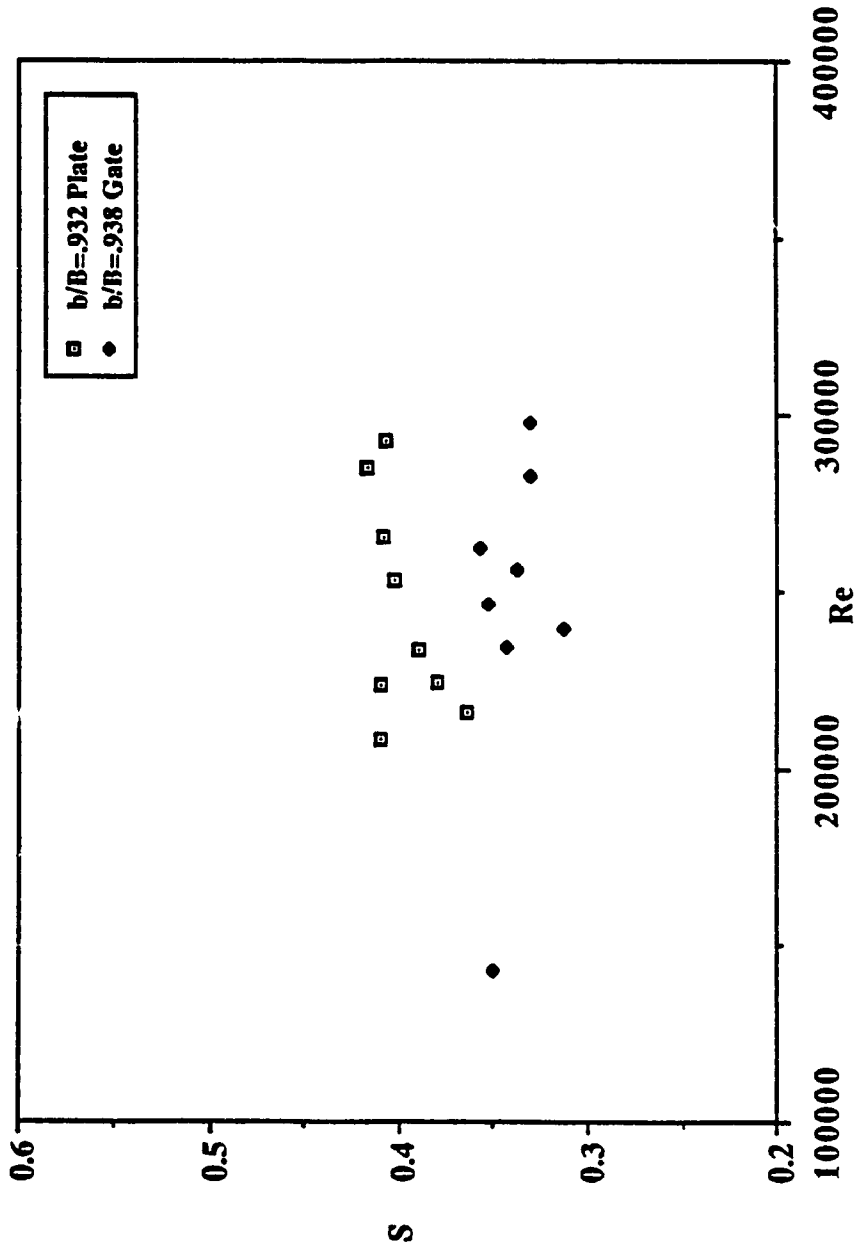

Fig. 11 Variation of S with Re for flat plate and gate

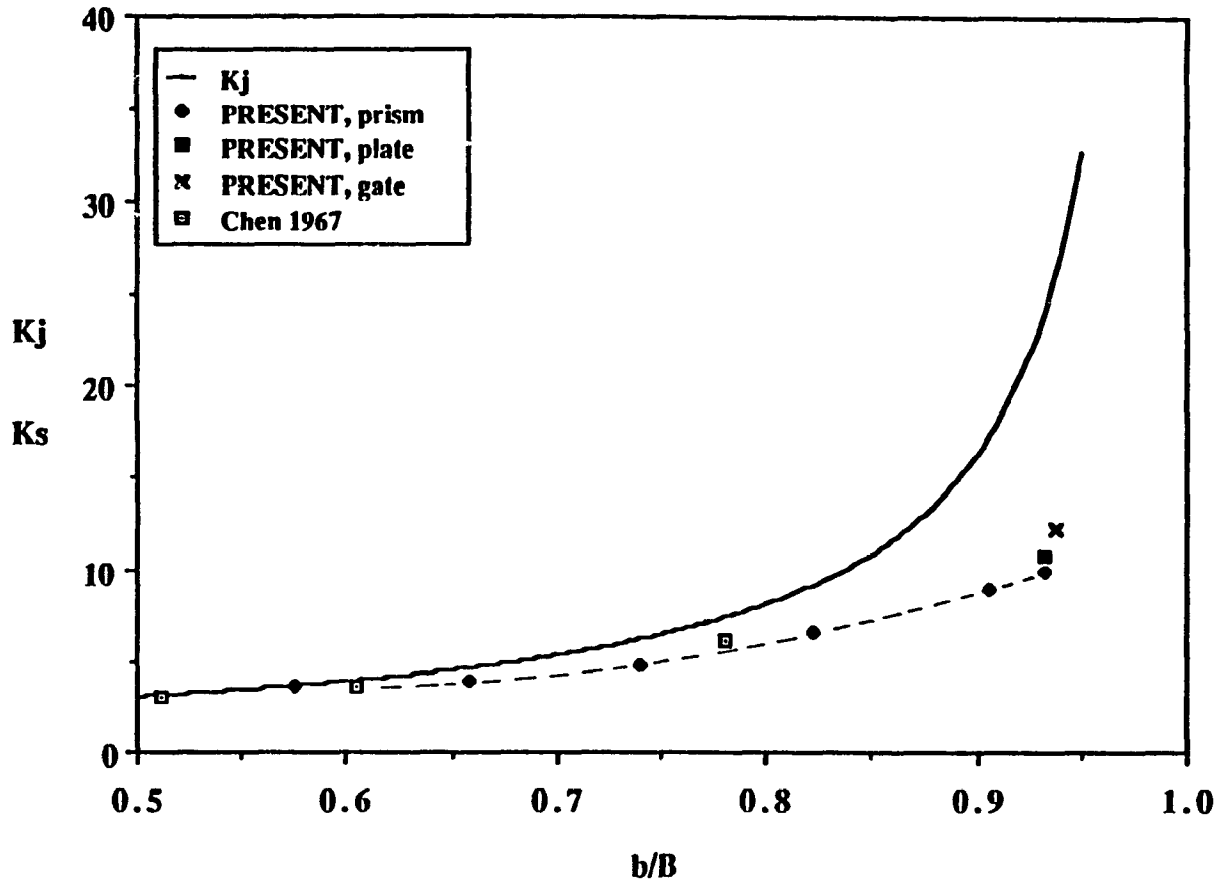

Fig. 12 Variation of K_j and K_s with blockage for sharp-edged bluff bodies ($b/B > 0.5$)

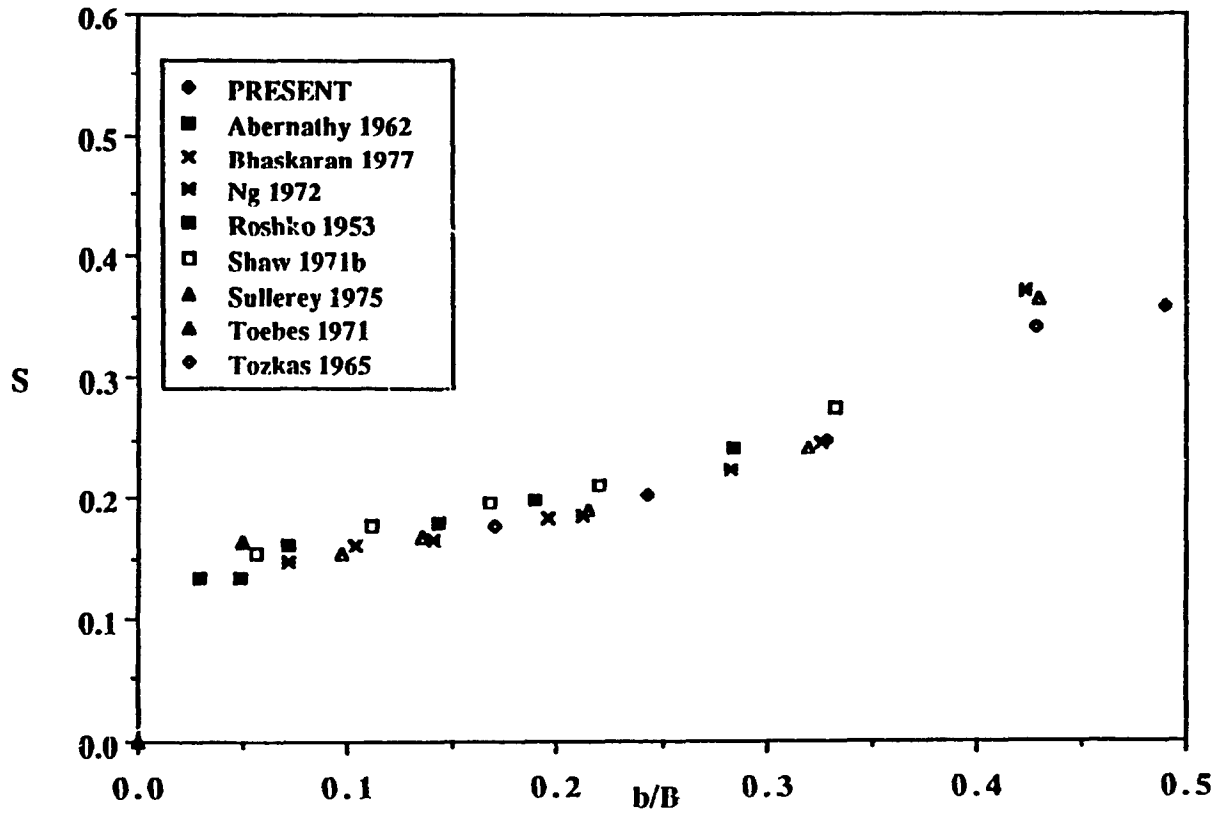

Fig. 13 Variation of S with blockage for 0° prism (b/B < 0.5)

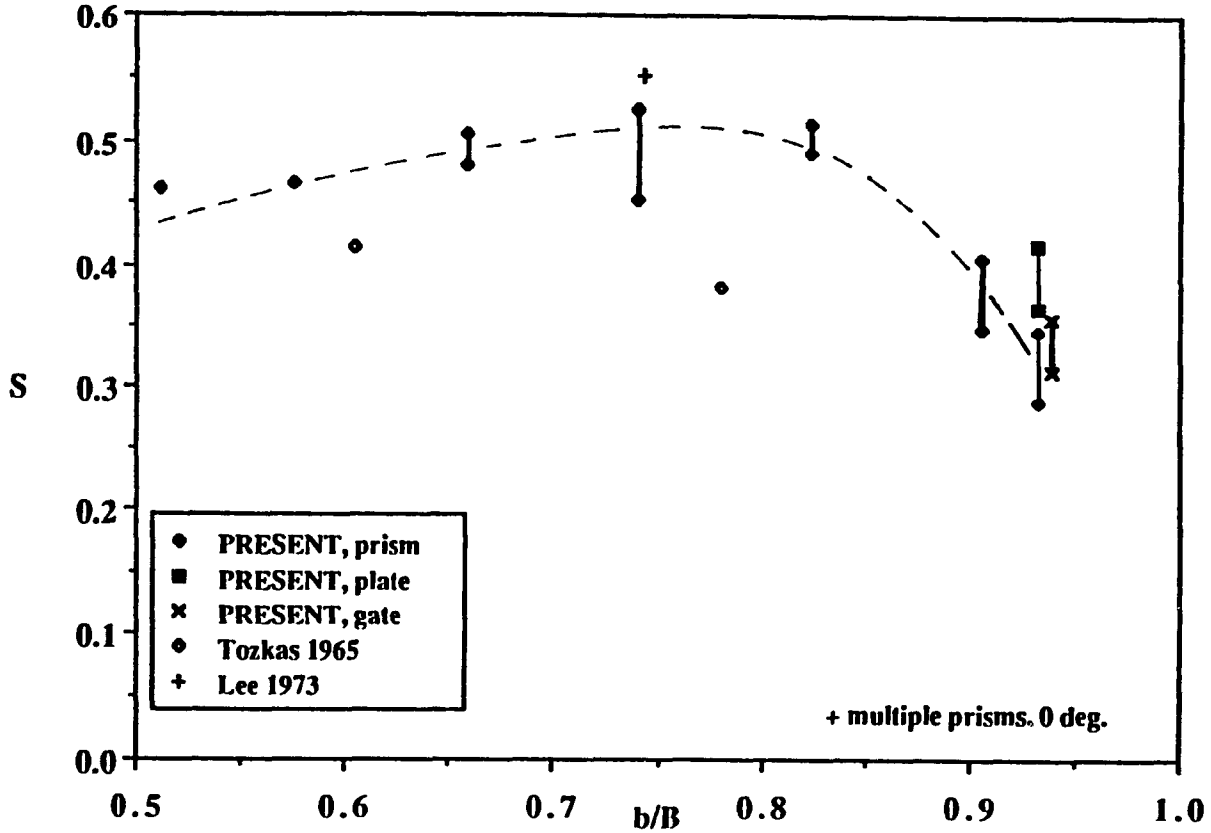

Fig. 14 Variation of S with blockage for 0° prism (b/B > 0.5)

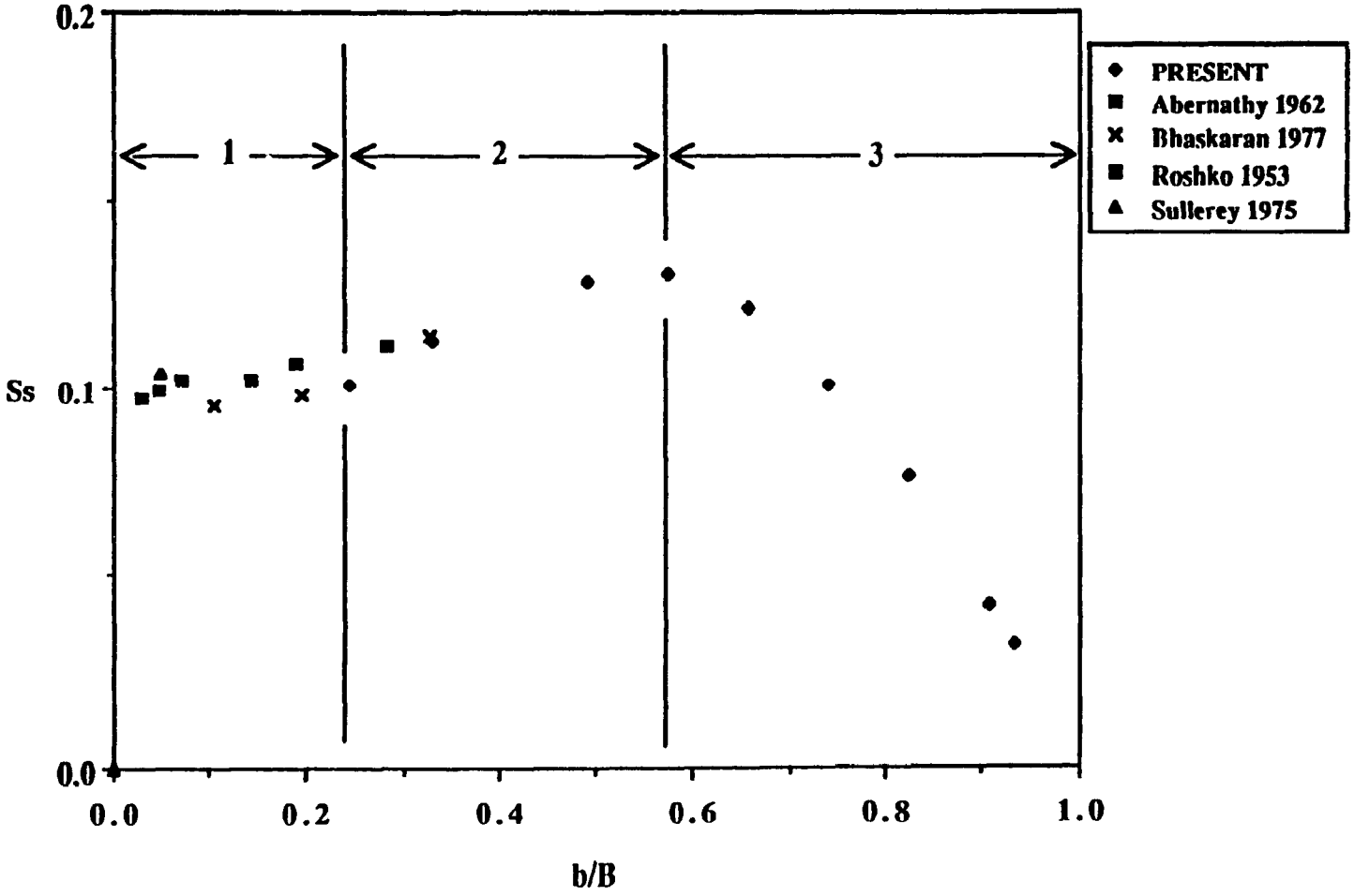

Fig.15 Variation of S_s with blockage for sharp-edged bluff bodies
($0 < b/B < 1.0$)
1 - Mildly constrained
2 - Moderately constrained
3 - Highly constrained

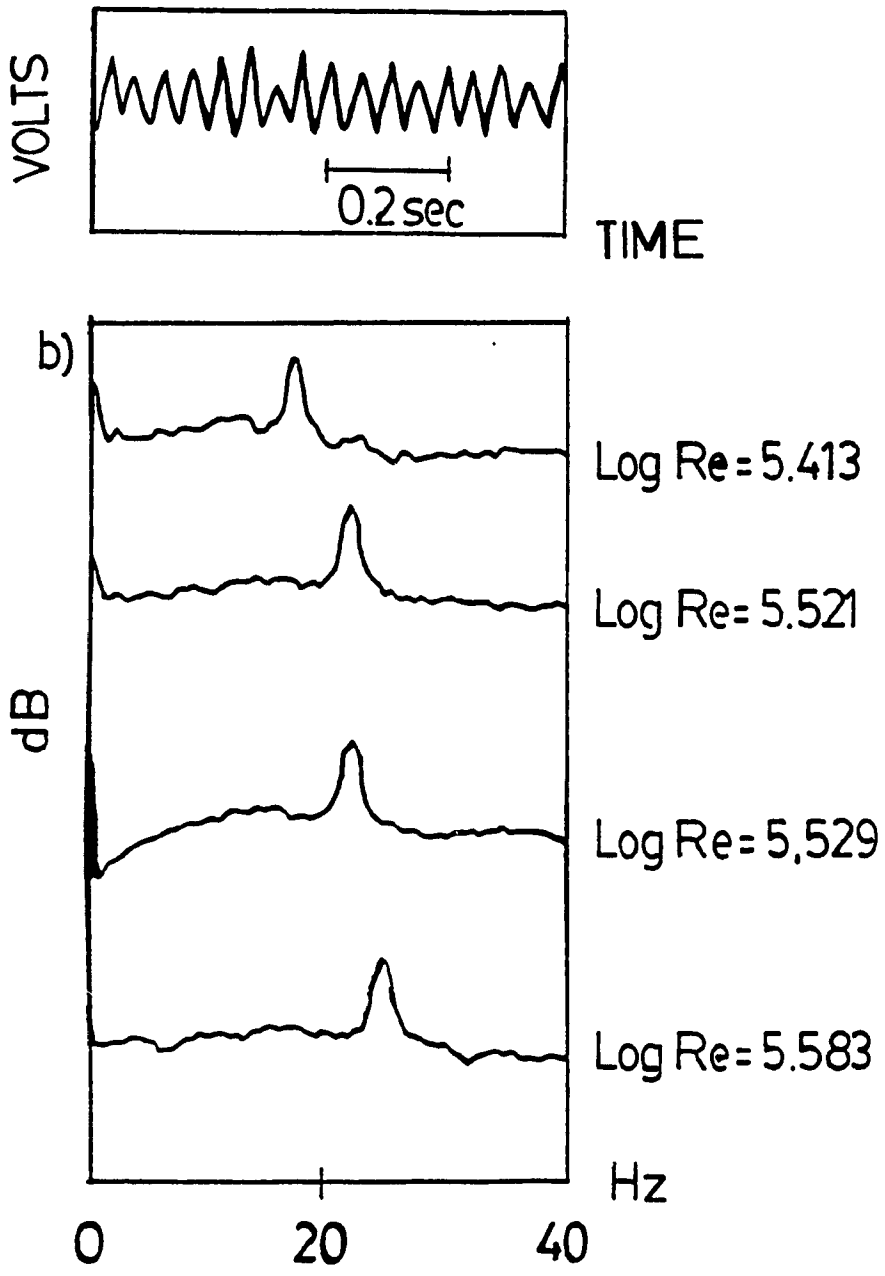

Fig.16 a) Typical pressure record for 0° prism (b/B=0.490)

b) Typical power spectra at various Re for 0° prism (b/B=0.490)

Note: Volts and dB are in arbitrary units

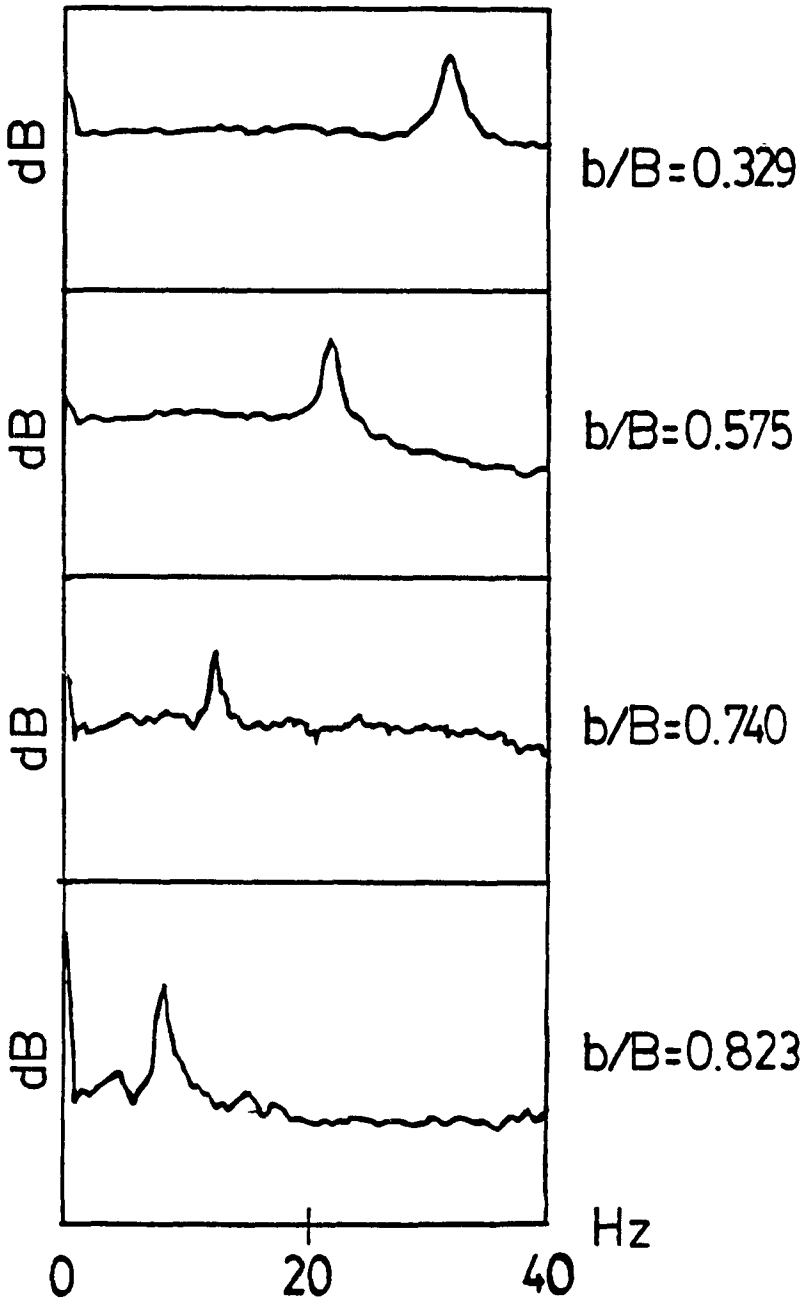

Fig. 17 Typical power spectra for 0° prism (b/B=0.329, 0.575, 0.740, 0.823)

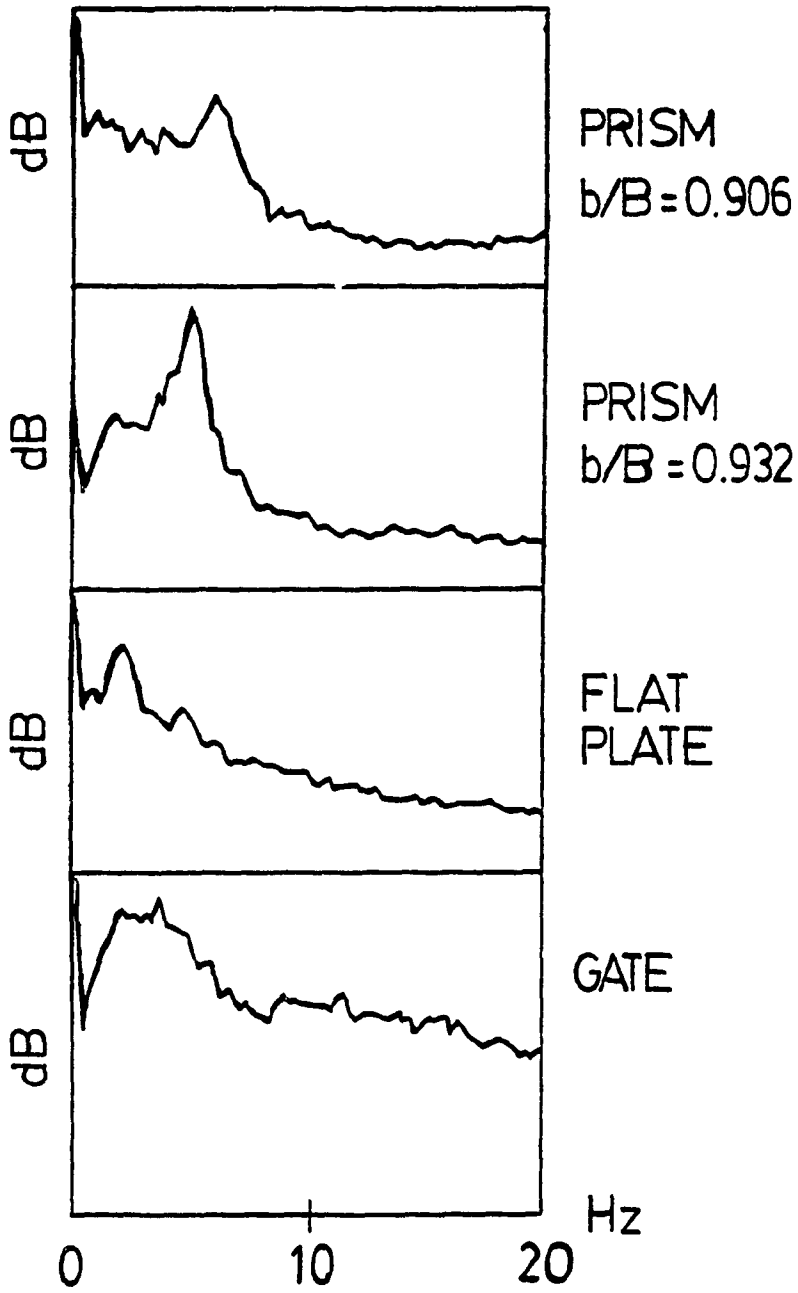

Fig. 18 Typical power spectra for 0° prism (b/B=0.906, 0.932) and for flat plate and gate

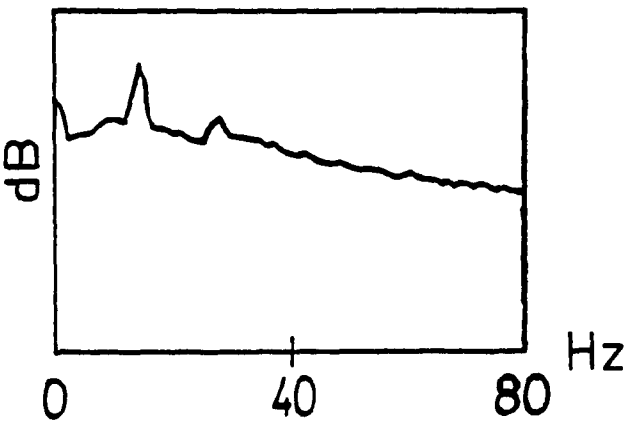

Fig. 19 Typical power spectra for 0° prism (b/B=0.658)

TABLE 1: Comprehensive table of separation pressure coefficient and Strouhal number for sharp-edged bluff bodies

Author	b/B	S	K_s	$-C_{ps}$	C_d	Log Re	Remarks
Abernathy (1962)	0.071 0.143 0.189 0.284	0.161 0.179 0.198 0.244	1.58 1.75 1.85 2.18	1.50 2.02 2.42 3.75			Flat plate
Awbi (1978)	0.051		1.56	1.43	2.14	4.792-5.090	Flat plate
Bhaskaran (1977)	0.103 0.196 0.326	0.160 0.183 0.248	1.69 1.84 2.16	1.85 2.38 3.65	2.77 3.77 4.38		Triangular 0 deg. prism. Data at high cavitation number
Chen (1967)	0.170 0.429 0.512 0.605 0.780		1.88 2.64 3.02 3.66 6.12	2.54 5.98 8.11 12.40 36.40			Flat plate
Courchesne and Laneville (1979)	0.063		1.73	2.00	2.71	4.301-5.000	Rectangular cylinder
Lee (1973)	0.186 0.243 0.324		1.79 1.99 2.22	2.19 2.96 3.95	3.38 3.81 4.91	4.613-4.863	Triangular 0 deg prism
Modi and El-Shirbiny (1977)	0.090 0.205 0.355		1.58 1.87 2.22	1.50 2.50 3.95	2.20 3.00 4.60		Flat plate
Ng (1972)	0.071 0.141 0.212 0.282 0.423 0.564 0.705	0.148 0.166 0.185 0.223 0.371			2.38 2.83 3.63 4.34 7.50 14.46 34.43	4.086-5.365	Triangular 0 deg. prism

TABLE 1: Comprehensive table of separation pressure coefficient and Strouhal number for sharp-edged bluff bodies (continued)

Author	b/B	S	K_s	$-C_{ps}$	C_d	Log Re	Remarks
Roshko (1953)	0.029 0.048	0.135 0.134	1.39 1.36	0.93 0.86		3.480- 4.225	Flat plate (mean values)
Shaw (1969)	0.132		1.68	1.82			Flat plate
Shaw (1971a)	0.132				2.48		Flat plate
Shaw (1971b)	0.056 0.111 0.167 0.220 0.332	0.155 0.177 0.196 0.210 0.275					Flat plate
Simmons (1974)	0.035		1.54	1.37		4.176	Flat plate
Sullerey et. al. (1975)	0.050	0.162	1.56	1.44		4.061	Flat plate
Toebes (1971)	0.097 0.135 0.215 0.320 0.430	0.155 0.167 0.190 0.243 0.365					Triangular 0 deg. prism
Tozkas (1965)	0.170 0.429 0.512 0.605 0.780	0.177 0.341 0.460 0.415 0.382					Flat plate

TABLE 2*: Variation of separation pressure coefficient and Strouhal number with Reynolds number for 0 deg. prism (b/B=0.243)

b/B	Log Re	$P_{u/s}$ (psi)	u (fps)	$-C_{ps}$	S
0.243	5.332	6.9	17.77	3.11	0.204
	5.350	6.9	18.52	3.00	0.204
	5.364	10.2	19.10	3.09	0.203
	5.371	13.7	19.40	3.04	0.202
	5.393	14.6	20.40	3.02	0.200
	5.524	36.4	27.54	2.89	0.196

TABLE 3*: Variation of separation pressure coefficient and Strouhal number with Reynolds number for 0 deg. prism (b/B=0.329)

b/B	Log Re	$P_{u/s}$ (psi)	u (fps)	$-C_{ps}$	S
0.329	5.375	5.7	14.09	4.26	0.259
	5.447	9.5	16.66	4.05	0.255
	5.481	19.8	18.05	3.99	0.252
	5.501	21.6	18.86	3.82	0.251
	5.507	22.2	19.10	3.78	0.250
	5.509	18.7	19.25	3.95	0.251
	5.549	27.0	21.07	3.74	0.249
	5.551	26.5	21.22	3.80	0.247
	5.583	33.5	22.82	3.73	0.247
	5.598	38.4	23.59	3.88	0.245
	5.606	36.6	24.04	3.70	0.244
	5.635	43.0	25.75	3.81	0.244

* Present investigation

TABLE 4*: Variation of separation pressure coefficient and Strouhal number with Reynolds number for 0 deg. prism (b/B=0.490)

b/B	Log Re	$P_{u/s}$ (psi)	u (fps)	$-C_{ps}$	S
0.490	5.413	16.1	11.56	6.82	0.362
	5.446	15.0	12.44	6.91	0.363
	5.521	10.5	14.80	7.18	0.362
	5.529	9.9	15.05	7.24	0.362
	5.583	13.2	17.07	6.89	0.357
	5.680	17.4	21.34	6.66	0.348

TABLE 5*: Variation or separation pressure coefficient and Strouhal number with Reynolds number for 0 deg. prism (b/B=0.575)

b/B	Log Re	$P_{u/s}$ (psi)	u (fps)	$-C_{ps}$	S
0.575	5.330	6.2	8.33	12.33	0.478
	5.336	4.9	8.57	12.20	0.475
	5.474	9.3	11.77	11.49	0.457
	5.491	10.9	12.22	11.70	0.462
	5.512	17.2	13.45	11.54	0.461
	5.515	13.3	13.53	11.88	0.464

* Present investigation

TABLE 6*: Variation of separation pressure coefficient and Strouhal number with Reynolds number for 0 deg. prism (b/B=0.658)

b/B	Log Re	$P_{u/s}$ (psi)	u (fps)	$-C_{ps}$	S
0.658	5.318	5.2	6.35	17.11	0.498
	5.396	7.4	7.58	16.14	0.488
	5.401	6.6	7.69	15.39	0.485
	5.430	8.6	8.57	14.46	0.506
	5.481	15.9	9.66	14.36	0.492
	5.525	19.6	10.67	14.85	0.486
	5.560	22.1	11.56	13.51	0.481
	5.574	24.1	11.94	14.70	0.485

TABLE 7*: Variation of separation pressure coefficient and Strouhal number with Reynolds number for 0 deg. prism (b/B=0.740)

b/B	Log Re	$P_{u/s}$ (psi)	u (fps)	$-C_{ps}$	S
0.740	5.305	5.4	5.48	22.81	0.526
	5.394	8.5	6.71	22.83	0.496
	5.476	11.6	8.10	22.45	0.481
	5.537	14.4	9.32	22.39	0.482
	5.746	35.8	15.09	20.30	0.453

* Present investigation

TABLE 8*: Variation of separation pressure coefficient and Strouhal number with Reynolds number for 0 deg. prism (b/B=0.823)

b/B	Log Re	$P_{u/s}$ (psi)	u (fps)	$-C_{ps}$	S
0.823	5.360	10.5	5.91	42.56	0.511
	5.408	19.4	6.62	41.62	0.491
	5.427	23.1	6.89	40.85	0.499
	5.435	27.6	7.04	40.79	0.516
	5.505	26.5	10.03	41.38	0.506
	5.558	27.6	9.06	42.42	0.506

TABLE 9*: Variation of separation pressure coefficient and Strouhal number with Reynolds number for 0 deg. prism (b/B=0.906)

b/B	Log Re	$P_{u/s}$ (psi)	u (fps)	$-C_{ps}$	S
0.906	5.149	7.4	3.35	78.67	0.376
	5.253	10.7	4.24	78.67	0.367
	5.394	32.0	5.91	76.73	0.407
	5.398	34.7	5.95	76.21	0.347
	5.413	37.5	6.16	76.35	0.372
	5.476	29.7	7.12	78.37	0.386

* Present investigation

TABLE 10*: Variation of separation pressure coefficient andStrouhal number with Reynolds number for 0 deg. prism (b/B=0.932)

b/B	Log Re	$P_{u/s}$ (psi)	u (fps)	$-C_{ps}$	S
0.932	5.241	19.0	4.02	100.69	0.339
	5.260	21.0	4.22	100.50	0.323
	5.276	16.8	4.37	98.51	0.311
	5.286	17.7	4.46	98.31	0.332
	5.299	24.6	4.61	98.93	0.322
	5.328	39.1	4.93	97.75	0.345
	5.334	28.2	4.99	96.44	0.321
	5.367	31.1	5.38	95.59	0.317
	5.380	34.9	5.56	95.60	0.328
	5.403	37.3	5.84	97.14	0.313
	5.413	38.9	5.98	97.13	0.304
	5.423	43.1	6.13	95.36	0.319
	5.435	46.0	6.28	95.48	0.311
	5.459	42.8	6.65	94.72	0.310
	5.489	33.0	7.12	94.92	0.289

* Present investigation

TABLE 11*: Variation of separation pressure coefficient and Strouhal number with Reynolds number for flat plate (b/B=0.932)

b/B	Log Re	$P_{u/s}$ (psi)	u (fps)	$-C_{ps}$	S
0.932	5.318	23.9	4.43	111.83	0.411
	5.334	19.0	4.67	120.23	0.365
Flat	5.348	28.9	4.74	119.74	0.411
plate	5.350	34.0	4.80	117.27	0.381
	5.367	29.3	4.99	116.21	0.391
	5.403	46.3	5.42	112.67	0.403
	5.423	36.2	5.59	119.69	0.409
	5.455	40.8	6.02	114.50	0.418
	5.467	43.5	6.20	114.45	0.408

TABLE 12*: Variation of separation pressure coefficient and Strouhal number with Reynolds number for gate (b/B=0.938)

b/B	Log Re	$P_{u/s}$ (psi)	u (fps)	$-C_{ps}$	S
0.938	5.155	10.4	2.86	167.84	0.350
	5.369	30.6	4.64	149.53	0.344
Gate	5.378	23.2	4.74	150.34	0.313
	5.391	24.1	4.89	146.38	0.353
	5.408	26.2	5.09	148.10	0.338
	5.418	35.2	5.15	149.96	0.357
	5.452	40.7	5.56	147.26	0.330
	5.474	35.0	5.95	145.99	0.330

* Present investigation

APPENDIX I

EXPERIMENTAL UNCERTAINTIES

Title	Error range
Test models	Linear measurement ± 0.02 mm
Test section	Linear measurement ± 0.02 mm
Pressure	± 0.1 psi
Separation pressure coefficient	± 0.03
Strouhal number	± 0.02
Discharge	± 3.0 %
Temperature	± 0.5° C